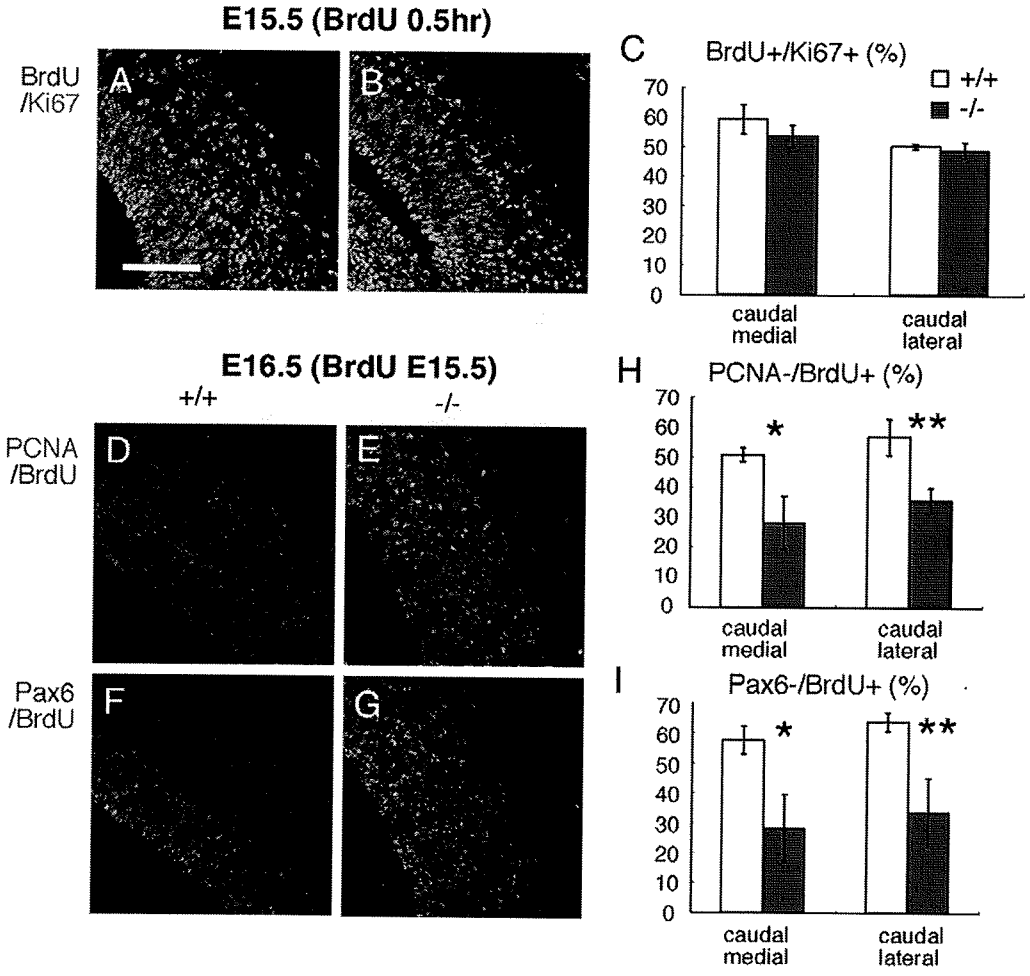

Fig. 9. Impairment of cell-cycle exit in the *RP58*-deficient cortex in late neocortical development. (A–C) Double labeling with BrdU and Ki67 in the lateral region of the wild-type (A) and mutant (B) caudal neocortex at E15.5, 0.5 h after BrdU incorporation. The fraction of BrdU-positive cells among the Ki67-positive cells was not altered in the medial and lateral regions of the mutant cortex (C), which suggests that proliferation is not affected in the mutant cortex. Fifty Ki67-positive cells were randomly examined. Four regions of two mutant brains were compared with six regions of three wild-type brains. (D–I) BrdU was incorporated at E15.5 and the lateral region of the caudal neocortex was double stained for BrdU and PCNA (D and E) or Pax6 (F and G) in the lateral region of the wild-type (D and F) and the mutant (E and G) at E16.5. The fraction of PCNA-negative cells and Pax6-negative cells among the BrdU-positive cells was reduced in the caudal *RP58*-deficient cortex in both the medial and lateral regions of the mutant caudal neocortex (H and I), which suggests that cell-cycle exit was reduced. Fifty BrdU-positive cells were randomly examined. Three regions of three mutant brains were compared with three regions of three wild-type brains. Scale bar, 0.1 mm (A–D, G, and H). The data are presented as means ± SD. *$P<0.02$, **$P<0.01$ (Student's t test).

of cell-cycle exit only at late embryonic stages and/or the presence of high levels of apoptosis in the *RP58*$^{-/-}$ cortex. We consider RP58 a candidate molecule for the control of the number of mature cortical neurons, as *RP58* deficiency decreased the number of mature neurons because of enhanced apoptosis and of defects in cell-cycle exit.

A delicate balance in cell proliferation and subsequent cell-cycle withdrawal and differentiation into specific neurons is essential for corticogenesis. The present study indicates the possibility that RP58 regulates this balance, at least at the late embryonic stage. In the wild-type E15.5 VZ, some RP58-positive cells showed weak Pax6 immunoreactivity, and almost all RP58-positive cells exhibited Tbr2 immunoreactivity (Supplementary Fig. 9), which suggests that the onset of RP58 expression happens in IMPs, at the initial stage, when Pax6 and Tbr2 may be coexpressed (Englund et al., 2005).

Pax6+ cells were increased in the *RP58* null mutant, as were both Pax6+/Tbr2− and Pax6+/Tbr2+ cells. The increase in the number of Pax6+/Tbr2− cells in the mutant is explained by the reduction of cell-cycle exit of VZ progenitors. It is likely that there are extrinsic actions that allow RP58 to activate the expression of extrinsic factors that control cell-cycle exit, because RP58 is not detected in most Pax6+ cells. In fact, it is reported that the generation of projection neurons from cortical progenitors appears to be governed by both cell-intrinsic and environmental cues (Mizutani and Gaiano, 2006); however, we cannot exclude the possibility that a few Pax6+ cells abnormally proliferated in the mutant, as RP58 was detected in some Pax6+ cells in the wild type.

Pax6+/Tbr2− and Pax6+/Tbr2+ cells were increased in the mutant VZ/SVZ, whereas Pax6−/Tbr2+ cells were not increased. Therefore, it is possible that Pax6 is ectopically expressed in Tbr2+ IMPs in the mutant, and that the transition from Pax6+/Tbr2+ cells to Pax6−/Tbr2+ cells was inhibited in the mutant, which raises the possibility that RP58 may be an important molecule for the maturation of IMPs. It was reported that (1) Svet1 is a spliced intronic sequence from Unc5d (Sasaki et al., 2008) and (2) Svet1/Unc5d staining is a specific marker of late-stage IMPs. It is likely that Svet1/Unc5d expression was reduced in the mutant, which supports the possibility that RP58 is most important for maturation process from early-stage IMPs to late-stage IMPs; however, as the expression of Svet1/Unc5d is also observed in young neurons (Kawaguchi et al., 2008), the possibility that the reduction of Svet1/Unc5d signal in the mutant reflects the reduction of the number of generated neurons cannot be excluded.

The expression of Pax6, Tbr2, and Svet1/Unc5d reveals that the formation of VZ/SVZ was impaired in the mutant (Supplementary Figs. 15 and 16). The outer Pax6-dominant zone in the E16.5 mutant may be caused by the reduced cell-cycle exit (Supplementary Fig. 18). The outer Pax6-dominant zone in E16.5 was not distinct when compared with that of the E18.5 animals. Therefore, the outer Pax6-dominant zone observed in the E18.5 mutant may partially explain the reduced cell-cycle exit.

Tbr2-positive cells were increased in the mutant VZ/SVZ, as were Pax6+/Tbr2+ cells, but not Pax6−/Tbr2+ cells. Tbr2+ IMPs are originated from Pax6+ RGPs. Therefore, the increase in Pax6+/Tbr2+ cells in the mutant may be explained by the increase in Pax6+/Tbr2− cells.

We showed that RP58 was expressed in some Ngn2-positive cells (Supplementary Fig. 11). RP58 acts downstream of Ngn2 (Seo et al., 2007), which is involved in the initial commitment to a neuronal fate. Therefore, RGPs neuronally committed by Ngn2 probably express RP58 in the VZ in a sustained manner. As RP58 functions as a transcriptional repressor, it is possible that RP58 suppresses the expression of a few genes, which may include *Pax6*, *Tbr2*, and *Ngn2*. *In vitro* analysis indicated that the transcription of Ngn2 was suppressed by RP58 and that Ngn2-positive cells were increased in the *RP58*-null mutant cortex (data not shown; Ohtaka-Maruyama et al., in preparation). It was reported that Tbr2 is a target of Ngn2 (Ochiai et al., 2009). Therefore, the increase in Tbr2-positive cells in the *RP58* mutant can be explained by the enhancement of Ngn2 expression, probably because of a lack of transcriptional suppression by RP58.

On the other hand, the overexpression of some genes, which include *Pax6*, *Tbr2*, and *Ngn2*, may explain the abnormalities observed in the *RP58*-deficient brain. The overexpression of *Pax6* affects the proliferation of neuronal progenitors and causes failure of neuronal differentiation (Bel-Vialar et al., 2007) and Tbr2 misexpression inhibits cell-cycle exit (Sessa et al., 2008). We are now analyzing whether the phenotype of the *RP58* mutant brain can be explained by the enhanced expression of those genes.

In conclusion, we found that RP58 deficiency reduces the number of mature cortical neurons via strongly enhanced apoptosis and impaired cell-cycle exit, which suggests that RP58 plays a key role in the survival of cortical neurons and in the development of neuronal progenitors.

Acknowledgments

We thank Drs. Koki Kawamura, Makoto Hashimoto, Minoru Saitoe, Junjiro Horiuchi (Tokyo Metropolitan Institute for Neuroscience (TMIN)), Douglas E. Vetter (Tufts University School of Medicine), and Mitsuharu Hattori (Nagoya City University) for critical suggestions. We also thank Dr. Kazuaki Yoshikawa (Osaka University) for the guinea pig anti-Dlx2 antibody and Dr. David Anderson (California Institute of Technology) for the mouse anti-Neurogenin2 antibody. We thank Drs. Yoshinobu Sugitani and Tetsuo Noda (JFCR-Cancer Institute) for providing the mouse *CTGF*, mouse *Tailless*, mouse *Tbr1*, and mouse *SorLA* cDNAs used to prepare the probes for RNA *in situ* hybridization, as well as Dr. Thomas M. Jessell (Columbia University Medical Center) for mouse *ER81*, Dr. Susan K. McConnell (Stanford University) for mouse *RORβ*, Dr. Victor Tarabykin (Max Planck Institute of Biophysical Chemistry) for *Svet1*, Dr. Shinichi Aizawa (RIKEN Kobe) for *NT3*, Dr. Greg E. Lemke (Salk Institute) for *SCIP*, Dr. Jim Boulter (UCLA Brain Research and Molecular Biology Institutes) for *KA1*, and Dr. Francois Guillemot (NIMR) for *HES5* cDNAs. We also thank Ms. Yasuko Kishimoto (Histology Center, TMIN) for her technical assistance. These studies were supported by a grant-in-aid from the Ministry of Science, Education and Culture to H. O. and by Human Science Research Funds and the Budget for Nuclear Research of the MEXT, awarded to M. K.

Appendix A. Supplementary data

Supplementary data associated with this article can be found, in the online version, at doi:10.1016/j.ydbio.2009.04.030.

References

Allendoerfer, K.L., Shatz, C.J., 1994. The subplate, a transient neocortical structure: its role in the development of connections between thalamus and cortex. Annu. Rev. Neurosci. 17, 185–218.
Aoki, K., Meng, G., Suzuki, K., Takashi, T., Kameoka, Y., Nakahara, K., Ishida, R., Kasai, M., 1998. RP58 associates with condensed chromatin and mediates a sequence-specific transcriptional repression. J. Biol. Chem. 273, 26698–26704.
Arber, S., Ladle, D.R., Lin, J.H., Frank, E., Jessell, T.M., 2003. EST gene Er81 controls of formation of functional connection between group Ia sensory afferents and motor neurons. Cell 101, 485–498.
Bayer, S.A., Altman, J., 1991. Neocortical Development. Raven Press.
Buaas, F.W., Kirsh, A.L., Sharma, M., McLean, D.J., Morris, J.L., Griswold, M.D., de Rooji, D. G., Braun, R.E., 2004. Plzf is required in adult male germ cells for stem cell self-renewal. Nat. Genet. 36, 647–652.
Bel-Vialar, S., Medevielle, F., Pituello, F., 2007. The on/off of Pax6 controls the tempo of neuronal differentiation in the developing spinal cord. Dev. Biol. 305, 659–673.
Bettler, B., Boulter, J., Hermanss-Borgmeyer, U., Hollmann, M., Heinemann, S., 1990. Cloning of a novel glutamate receptor subunit, GluR5: expression in the nervous system during development. Neuron 5, 583–595.
Cau, E., Gradwohl, G., Casarosa, S., Kageyama, R., Guillemot, F., 2000. Hes genes regulate sequential stages of neurogenesis in the olfactory epithelium. Development 127, 2323–2332.
Chenn, A., Walsh, C.A., 2002. Regulation of cerebral cortical size by control of cell cycle exit in neural precursors. Science 297, 365–369.
Costoya, J.A., Hobbs, R.M., Barna, M., Cattoretti, G., Monava, K., Sukhwani, M., Orwig, K.E., Wolgemuth, D.J., Pandolfi, P.P., 2004. Essential role Plzf in maintenance of spermatogonial stem cells. Nat. Genet. 36, 653–659.
Dehay, C., Kennedy, H., 2007. Cell-cycle control and cortical development. Nat. Rev. Neurosci. 8, 438–450.
Englund, C., Fink, A., Lau, C., Pham, D., Daza, R.A.M., Bulfone, A., Kowalczyk, T., Hevner, R. F., 2005. Pax6, Tbr2, and Tbr1 are expressed sequentially by radial glia, intermediate progenitor cells, and postmitotic neurons in developing neocortex. J. Neurosci. 25, 247–251.
Forster, E., Zhao, S., Frotscher, M., 2006. Laminating the hippocampus. Nat. Rev. Neurosci. 7, 259–267.
Frantz, G.D., Bohner, A.P., Akers, R.M., McConnell, S.K., 1994. Regulation of the POU domain gene SCIP during cerebral cortical development. J. Neurosci. 14, 472–485.
Friedman, W.J., Ernfors, P., Persson, H., 1991. Transient and persistent expression of NT-3/HDNF mRNA in the rat brain during postnatal development. J. Neurosci. 11, 1577–1584.
Friedrichsen, S., Heuer, H., Christ, S., Winckler, M., Brauer, D., Bauer, K., Raivich, G., 2003. CTGF expression during mouse embryonic development. Cell Tissue Res. 312, 175–188.
Friocourt, G., Kanatani, S., Tabata, H., Yozu, M., Takahashi, T., Antypa, M., Raguénès, O., Chelly, J., Férec, C., Nakajima, K., Parnavelas, J.G., 2008. Cell-autonomous roles of ARX in cell proliferation and neuronal migration during corticogenesis. J. Neurosci. 28, 5794–5805.
Fuks, F., Burgers, W.A., Godin, N., Kasai, M., Kouzarides, T., 2001. Dnmt3a binds deacetylases and is recruited by a sequence-specific repressor to silence transcription. EMBO J. 10, 2536–2544.
Fukuda, T., Kawano, H., Ohyama, K., Li, H.P., Takeda, Y., Oohira, A., Kawamura, Y., 1997. Immunohistochemical localization of neurocan and L1 in the formation of thalamocortical pathway of developing rat. J. Comp. Neurol. 382, 141–152.
Funatsu, N., Inoue, T., Nakamura, S., 2004. Gene expression analysis of the late embryonic mouse cerebral cortex using DNA microarray: identification of several region- and layer-specific genes. Cereb. Cortex 14, 1031–1044.
Galichet, C., Guillemot, F., Parras, C.M., 2008. Neurogenin 2 has an essential role in development of the dentate gyrus. Development 135, 2031–2041.
Gebhardt, A., Kosan, C., Herkert, B., Möröy, T., Lutz, W., Eilers, M., Elsässer, H.P., 2007. Miz1 is required for hair follicle structure and hair morphogenesis. J. Cell. Sci. 120, 2586–2593.
Hashimoto, M., Rockenstein, E., Mante, M., Mallory, M., Masliah, E., 2001. β-synuclein inhibits α-synuclein aggregation: a possible role as an anti-parkinsonian factor. Neuron 32, 213–223.
Haubensak, W., Attardo, A., Denk, W., Huttner, W.B., 2004. Neurons arise in the basal neuroepithelium of the early mammalian telencephalon: a major site of neurogenesis. Proc. Natl. Acad. Sci. U. S. A. 101, 3196–3201.
Hermans-Borgmeyer, I., Hampe, W., Schinke, B., Methner, A., Nykjaer, A., Süsens, U., Fenger, U., Herbarth, B., Schaller, H.C., 1998. Unique expression pattern of a novel mosaic receptor in the developing cerebral cortex. Mech. Dev. 70, 65–76.
Heuer, H., Christ, S., Friedrichsen, S., Brauer, D., Winckler, M., Bauer, K., Raivich, G., 2003. Connective tissue growth factor: a novel marker of layer VII neurons in the rat cerebral cortex. Neuroscience 119, 43–52.
Hevner, R.F., Hodge, R.D., Daza, R.A.M., Englund, C., 2006. Transcription factor in glutamatergic neurogenesis: conserved program in neocortex, cerebellum, and adult hippocampus. Neurosci. Res. 55, 223–233.
Ishida, R., Okado, H., Sato, H., Shionoiri, C., Aoki, K., Kasai, M., 2002. A role for the octameric ring protein, Translin, in mitotic cell division. FEBS Lett. 525, 105–110.

Kawaguchi, A., Ikawa, T., Kasukawa, T., Ueda, H.R., Kurimoto, K., Saitou, M., Matsuzaki, F., 2008. Single-cell gene profiling defines differential progenitor subclasses in mammalian neurogenesis. Development 135, 3113–3124.
Kawano, H., Fukuda, T., Kubo, K., Horie, M., Uyemura, K., Takeuchi, K., Osumi, N., Eto, K., Mawamura, K., 1999. Pax-6 is required for thalamocortical pathway formation in fetal rats. J. Com. Neurol. 408, 147–160.
Kelly, K.F., Daniel, J.M., 2006. POZ for effect-POZ-ZF transcription factors in cancer and development. Trends Cell Biol. 16, 578–587.
Kiefer, H., Chatail-Hermitte, F., Ravassard, P., Bayard, E., Brunet, I., Mallet, J., 2005. ZENON, a novel POZ Kruppel-like DNA binding protein associated with differentiation and/or survival of late postmitotic neurons. Mol. Cell. Biol. 25, 1713–1729.
Kuwajima, T., Nishimura, I., Yoshikawa, K., 2006. Necdin promotes GABAergic neuron differentiation in cooperation with Dlx homeodomain proteins. J. Neurosci. 26, 5383–5392.
Lee, S.M.K., Tole, S., Grove, E., McMahon, A.P., 2000. A local Wnt-3asignal is required for development of the mammalian hippocampus. Development 127, 457–467.
Li, G., Pleasure, S.J., 2007. Genetic regulation of dentate gyrus morphogenesis. Prog. Brain Res. 163, 143–152.
Martynoga, B., Morrison, H., David, J., Price, D.J., Mason, J.O., 2005. Foxg1 is required for specification of ventral telencephalon and region-specific regulation of dorsal telencephalic precursor proliferation and apoptosis. Dev. Biol. 283, 113–127.
Meng, G., Inazawa, J., Ishida, R., Tokura, K., Nakahara, K., Aoki, K., Kasai, M., 2000. Structural analysis of the gene encoding RP58, a sequence-specific transrepressor associated with heterochromatin. Gene 242, 59–64.
Meyer, G., Socorro, A.C., Garcia, C.G.P., Millan, L.M., Walker, N., Caput, D., 2004. Developmental roles of p73 in Cajal-Retzius cells and cortical patterning. J. Neurosci. 24, 9878–9887.
Miyata, T., Kawaguch, A., Saito, K., Kawano, M., Muto, T., Ogawa, M., 2004. Asymmetric production of surface-division and non-surface division cortical progenitor cells. Development 131, 3133–3145.
Mizutani, K., Gaiano, N., 2006. Chalk one up for 'nature' during neocortical neurogenesis. Nat. Neurosci. 9, 717–718.
Molyneaux, B.J., Arlotta, P., Menezes, J.R., Macklis, J.D., 2007. Neuronal subtype specification in the cerebral cortex. Nat. Rev. Neurosci. 8, 427–437.
Monaghan, A.P., Grau, E., Bock, D., Schutz, G., 1995. The mouse homolog of the orphan nuclear receptor tailless is expressed in the developing forebrain. Development 121, 839–853.
Nakajima, K., Mikoshiba, K., Miyata, T., Kudo, C., Ogawa, M., 1997. Disruption of hippocampal development in vivo by CR-50 mAb against Reelin. Proc. Natl. Acad. Sci. U. S. A. 94, 8196–8201.
Noctor, S.C., Martinez-Cerdeno, V., Ivic, L., Kringstein, A.R., 2004. Cortical neurons arise in symmetric and asymmetric division zones and migrate through specific phases. Nat. Neurosci. 7, 136–144.
Ochiai, W., Nakatani, S., Takahara, T., Kainuma, M., Masaoka, M., Minobe, S., Namihira, M., Nakashima, K., Sakakibara, A., Ogawa, M., Miyata, T., 2009. Periventricular notch activation and asymmetric Ngn2 and Tbr2 expression in pair-generated neocortical daughter cells. Mol. Cell Neurosci. 40, 225–233.
Ogawa, M., Miyata, T., Nakajimat, K., Yagyu, K., Seike, M., Ikenaka, K., Yamamoto, H., Mikoshiba, K., 1995. The *reeler* gene-associated antigen on Cajal-Retzius neurons is a crucial molecule for laminar organization of cortical neurons. Neuron 14, 899–912.
Ohtaka-Maruyama, C., Miwa, A., Kawano, H., Kasai, M., Okado, H., 2007. Spatial and temporal expression of RP58, a novel zinc finger transcriptional repressor, in mouse brain. J. Comp. Neurol. 502, 1098–1108.
Ohtsuka, T., Imayoshi, I., Shimojo, H., Nishi, E., Kageyama, R., McConnell, S., 2006. Visualization of embryonic neural stem cells using Hes promoters in transgenic mice. Mol. Cell. Neurosci. 31, 109–122.
Pleasure, S.J., Collins, A.E., Lowenstein, D.H., 2000. Unique expression pattern of cell fate molecule delinate sequential stages of dentate gyrus development. J. Neurosci. 20, 6095–6105.
Sasaki, S., Tabata, H., Tachikawa, K., Nakajima, K., 2008. The cortical subventricular zone-specific molecule Svet1 is part of the nuclear RNA coded by the putative Netrin receptor gene Unc5d and is expressed in multipolar migrating cells. Mol. Cell. Neurosci. 38, 474–483.
Seo, S., Lim, J.W., Yallajoshyula, D., Chang, L.W., Kroll, K.L., 2007. Neurogenin and NeuroD direct transcriptional targets and their regulatory enhancers. EMBO J. 26, 5093–5108.
Sessa, A., Mao, C.a., Hadjantonakis, A.K., Klein, W.H., Broccoli, V., 2008. Tbr2 directs conversion of radial glia into basal precursors and guides neuronal amplification by indirect neurogenesis in the developing neocortex. Neuron 60, 56–69.
Shinozaki, K., Yoshida, M., Nakamura, M., Aizawa, S., Suda, Y., 2004. Emx1 and Emx2 cooperate in initial phase of archipallium development. Mech. Dev. 121, 475–489.
Smart, I.H., McSherry, G.M., 1982. Growth patterns in the lateral wall of the mouse telencephalon. II. Histological changes during and subsequent to the period of isocortical neuron production. J. Anat. 34, 415–442.
Sugitani, Y., Nakai, S., Minowa, O., Nishi, M., Jishage, K., Kawano, H., Mori, K., Ogawa, M., Noda, T., 2002. Brn-1 and Brn-2 share crucial roles in the production and positioning of mouse neocortical neurons. Genes Dev. 16, 1760–1765.
Takahashi, A., Hirai, S., Ohtaka-Maruyama, C., Miwa, A., Hata, Y., Okabe, S., Okado, H., 2008. Co-localization of a novel transcriptional repressor simiRP58 with RP58. Biochem. Biophys. Res. Commun. 368, 637–642.
Tarabykin, V., Stoykova, A., Usman, N., Gruss, P., 2001. Cortical upper layer neurons derive from the subventricular zone as indicated by *Svet1* gene expression. Development 128, 1983–1993.
Weimann, J.M., Zhang, Y.A., Levin, M.E., Devin, W.P., Brulet, P., McConnell, S.K., 1999. Cortical neurons require Otx1 for the refinement of exuberant axonal projections to subcortical targets. Neuron 24, 819–831.

Activating Transcription Factor 3 Constitutes a Negative Feedback Mechanism That Attenuates Saturated Fatty Acid/Toll-Like Receptor 4 Signaling and Macrophage Activation in Obese Adipose Tissue

Takayoshi Suganami, Xunmei Yuan, Yuri Shimoda, Kozue Uchio-Yamada, Nobutaka Nakagawa, Ibuki Shirakawa, Takako Usami, Takamitsu Tsukahara, Keizo Nakayama, Yoshihiro Miyamoto, Kazuki Yasuda, Junichiro Matsuda, Yasutomi Kamei, Shigetaka Kitajima, Yoshihiro Ogawa

Abstract—Obese adipose tissue is markedly infiltrated by macrophages, suggesting that they may participate in the inflammatory pathways that are activated in obese adipose tissue. Evidence has suggested that saturated fatty acids released via adipocyte lipolysis serve as a naturally occurring ligand that stimulates Toll-like receptor (TLR)4 signaling, thereby inducing the inflammatory responses in macrophages in obese adipose tissue. Through a combination of cDNA microarray analyses of saturated fatty acid–stimulated macrophages in vitro and obese adipose tissue in vivo, here we identified activating transcription factor (ATF)3, a member of the ATF/cAMP response element-binding protein family of basic leucine zipper-type transcription factors, as a target gene of saturated fatty acids/TLR4 signaling in macrophages in obese adipose tissue. Importantly, ATF3, when induced by saturated fatty acids, can transcriptionally repress tumor necrosis factor-α production in macrophages in vitro. Chromatin immunoprecipitation assay revealed that ATF3 is recruited to the region containing the activator protein-1 site of the endogenous tumor necrosis factor-α promoter. Furthermore, transgenic overexpression of ATF3 specifically in macrophages results in the marked attenuation of proinflammatory M1 macrophage activation in the adipose tissue from genetically obese KKA^y mice fed high-fat diet. This study provides evidence that ATF3, which is induced in obese adipose tissue, acts as a transcriptional repressor of saturated fatty acids/TLR4 signaling, thereby revealing the negative feedback mechanism that attenuates obesity-induced macrophage activation. Our data also suggest that activation of ATF3 in macrophages offers a novel therapeutic strategy to prevent or treat obesity-induced adipose tissue inflammation. (***Circ Res.*** **2009;105:25-32.)**

Key Words: adipocytes ■ ATF3 ■ fatty acids ■ inflammation ■ macrophages ■ TLR4

Known as the metabolic syndrome, the cluster of well-established risk factors for cardiovascular disease (visceral fat obesity, impaired glucose metabolism, atherogenic dyslipidemia, and blood pressure elevation), is an increasing health problem worldwide.[1–3] The pathophysiology underlying the metabolic syndrome is not fully understood and visceral fat obesity appears to be an important component.[4] There is considerable evidence that obesity is a state of chronic low-grade inflammation, which may play a critical role in the pathophysiology of the metabolic syndrome.[1–3]

Obese adipose tissue is markedly infiltrated by macrophages, suggesting that they may participate in the inflammatory pathways that are activated in obese adipose tissue.[5] Using an in vitro coculture system composed of adipocytes and macrophages, we have provided evidence that a paracrine loop involving saturated fatty acids and tumor necrosis factor (TNF)α derived from adipocytes and macrophages, respectively, establishes a vicious cycle that augment the inflammatory change in obese adipose tissue.[6] Recent studies have also pointed to the heterogeneity of macrophages infiltrated into obese adipose tissue, ie, they follow 2 different polarization states: M1, or "classically activated" (proinflammatory) macrophages, which are induced by proinflammatory mediators such as lipopolysaccharide (LPS) and Th1 cytokine interferon-γ; and M2, or "alternatively activated" (antiinflammatory) macrophages, which are generated in vitro by expo-

Original received February 23, 2009; revision received May 11, 2009; accepted May 20, 2009.

From the Department of Molecular Medicine and Metabolism (T.S., X.Y., Y.S., N.N., I.S., Y.K., Y.O.), Department of Biochemical Genetics (S.K.), Global Center of Excellence Program (Y.O.); and International Research Center for Molecular Science in Tooth and Bone Diseases, Laboratory of Recombinant Animals (T.U.), Medical Research Institute, Tokyo Medical and Dental University, Tokyo; Division of Biomedical Research Resources (K.U.-Y., J.M.), National Institute of Biomedical Innovation, Osaka; Kyoto Institute of Nutrition and Pathology (T.T., K.N.); Department of Medicine (Y.M.), Division of Atherosclerosis and Diabetes, National Cardiovascular Center Hospital, Osaka; and Department of Metabolic Disorder (K.Y.), Research Institute, International Medical Center of Japan, Tokyo, Japan.

Correspondence to Yoshihiro Ogawa, Department of Molecular Medicine and Metabolism, Medical Research Institute, Tokyo Medical and Dental University, 1-5-45 Yushima, Bunkyo-ku, Tokyo 113-8510, Japan. E-mail ogawa.mmm@mri.tmd.ac.jp

Circulation Research **is available at http://circres.ahajournals.org** **DOI: 10.1161/CIRCRESAHA.109.196261**

sure to Th2 cytokines such as interleukin (IL)-4 and IL-13.[7–9] Evidence has accumulated indicating that macrophages, which are infiltrated into obese adipose tissue, exhibit the phenotypic change from M2 to M1 polarization.[7–9] Recent evidence also showed that the nuclear receptor peroxisome proliferator-activated receptor-γ or -δ regulates M2 polarization of adipose tissue macrophages and thus systemic insulin sensitivity.[8,9] It is, therefore, conceivable that M1 macrophages induce the release of saturated fatty acids from hypertrophied adipocytes via lipolysis, which, in turn, may serve as a proinflammatory adipocytokine locally in the adipose tissue.

Free fatty acids represent an important energy source mobilized from triglycerides stored in the adipose tissue, particularly during periods of starvation, but recent evidence has suggested the pathophysiologic roles other than the supply of nutrients in times of fasting or increased energy demand.[10] For instance, elevated levels of circulating free fatty acids, which are often associated with visceral fat obesity, increase fat accumulation in insulin target tissues such as the skeletal muscle and liver and contribute to insulin resistance.[11] We and others have reported that saturated fatty acids, which are released from adipocytes via the macrophage-induced lipolysis, serve as a naturally occurring ligand for Toll-like receptor (TLR)4 complex, which is essential for the recognition of LPS, to induce nuclear factor (NF)-κB activation in macrophages.[12–14] Evidence has also suggested that TLR4 plays an important role in adipose tissue inflammation.[14–17] Because macrophages in obese adipose tissue are exposed to saturated fatty acids released in large quantities from hypertrophied adipocytes, there might be negative regulatory mechanisms, whereby macrophages are protected against the saturated fatty acid–induced inflammatory response in obese adipose tissue.

Through a combination of cDNA microarray analyses of saturated fatty acid–stimulated macrophages in vitro and obese adipose tissue in vivo, we identified activating transcription factor (ATF)3, a member of the ATF/cAMP response element-binding protein (CREB) family of basic leucine zipper-type transcription factors[18,19] that is markedly induced in macrophages through TLR4 in response to saturated fatty acids in vitro and in obese adipose tissue in vivo. This study provides evidence that ATF3 acts as a transcriptional repressor of saturated fatty acids/TLR4 signaling in macrophages, thereby revealing the negative feedback mechanism that attenuates obesity-induced macrophage activation in obese adipose tissue. Our data also suggest that activation of ATF3 in macrophages offers a novel therapeutic strategy to prevent or treat obesity-induced inflammation and thus the metabolic syndrome associated with excess adiposity.

Materials and Methods

An expanded Materials and Methods section is available in the Online Data Supplement at http://circres.ahajournals.org.

Materials and Antibodies

Details are provided in the Online Data Supplement.

Animals

Six-week-old male C3H/HeJ mice, which have defective LPS signaling attributable to a missense mutation in the TLR4 gene,[20] and control C3H/HeN mice were purchased from CLEA Japan (Tokyo, Japan). Genetically obese *ob/ob*, *db/db*, and KKA^y mice were purchased from CLEA Japan and Charles River Japan (Tokyo, Japan). Details on experimental conditions are provided in the Online Data Supplement. All animal experiments were conducted in accordance to the guidelines of Tokyo Medical and Dental University Committee on Animal Research (No. 0090058).

Generation of Transgenic Mice Overexpressing ATF3 in Macrophages

Details are provided in the Online Data Supplement.

Cell Culture

RAW264 macrophage cell line (RIKEN BioResource Center, Tsukuba, Japan), 3T3-L1 preadipocytes, and HEK293 (American Type Culture Collection, Manassas, Va) were maintained in DMEM (Nacalai Tesque, Kyoto, Japan) containing 10% FBS (BioWest, Miami, Fla). Differentiation of 3T3-L1 preadipocytes to mature adipocytes was performed as previously described[6,12] and used as differentiated 3T3-L1 adipocytes at days 8 to 10 after the induction of differentiation. Murine peritoneal macrophages and bone marrow–derived macrophages were prepared as described.[12]

Chromatin Immunoprecipitation Assay

Details are provided in the Online Data Supplement.

Retrovirus-Mediated Overexpression and Knockdown of ATF3 in Macrophages

Retrovirus-mediated overexpression of the full-length mouse ATF3 cDNA and knockdown of endogenous ATF3 were performed in RAW264 macrophages as described in the Online Data Supplement.

Quantitative Real-Time PCR

Total RNA was extracted from cultured cells using Sepazol reagent (Nacalai Tesque) and quantitative real-time PCR was performed with an ABI Prism 7000 Sequence Detection System using PCR Master Mix Reagent (Applied Biosystems, Foster City, Calif).[6,12] Primers used in this study are described in Online Table I. Levels of mRNA were normalized to those of 36B4 mRNA.

Histological Analysis

Histological analysis was performed as previously described using the paraffin-embedded sections of the epididymal white adipose tissue.[15] In brief, hematoxylin/eosin staining was used to compare the adipocyte cell size with the software Win Roof (Mitani, Chiba, Japan).[15] The presence of F4/80-positive macrophages in the adipose tissue was detected immunohistochemically using the rat monoclonal antimouse F4/80 antibody[21] as described previously.[15] The number of F4/80-positive cells was counted in more than 10 mm^2 area of each section and expressed as the mean number/mm^2.

Western Blotting of ATF3

Whole cell lysates were prepared as previously described.[6] Samples (20 μg protein per lane) were separated by 12.5% SDS-PAGE and Western blotting was performed using antibodies against ATF3 (Santa Cruz Biotechnology).

Measurement of TNFα Levels in Culture Media

The TNFα levels in culture supernatants were determined by a commercially available ELISA kit (R&D systems, Minneapolis, Minn).[6]

Transient Transfection and Luciferase Assay

Details are provided in the Online Data Supplement.

Statistical Analysis

Data were expressed as the means±SE. Statistical analysis was performed using ANOVA, followed by Scheffe's test unless otherwise described. $P<0.05$ was considered to be statistically significant.

Results and Discussion

Identification of ATF3 As a Target Gene of Saturated Fatty Acids in Macrophages in Obese Adipose Tissue

We have provided in vitro evidence that saturated fatty acids, which are released from adipocytes via the macrophage-induced lipolysis, serves as a naturally occurring ligand that stimulates TLR4 signaling in macrophages.[12] To search for target gene(s) of saturated fatty acids in macrophages in obese adipose tissue, we performed cDNA microarray analysis of obese adipose tissue from *ob/ob* mice and palmitate-stimulated RAW264 macrophages (Online Figure I, a). Upregulated genes under both conditions included chemokines, proinflammatory cytokines, acute phase reactants, and ATF3 (Online Table II), whereas 5 genes were downregulated (Online Table III). ATF3 is a member of the ATF/CREB family of transcription factors.[18,19] ATF3 is rapidly induced in response to several stimuli and insults, such as chemicals, irradiation, and oxidative stress, and, in turn, negatively regulates target genes as a transcriptional repressor.[18,19] Although ATF3 plays a role in apoptosis and cell cycle,[18,19,22] the role of ATF3 in obesity is largely unknown. We, therefore, investigated the tissue distribution of ATF3 in obese and lean mice. Similar to macrophage marker F4/80, ATF3 mRNA expression was markedly increased in the adipose tissue from *db/db* mice relative to wild-type mice (Online Figure I, b). In this study, there was a significant increase in ATF3 mRNA expression in the liver from *db/db* mice relative to wild-type mice ($P<0.01$).

We confirmed our cDNA microarray data by real-time PCR and immunostaining. Expression of ATF3 and F4/80 mRNAs was increased in the adipose tissue during the course of diet-induced obesity (Figure 1A). We also observed upregulation of ATF3 and F4/80 in the adipose tissue from *ob/ob* mice (Figure 1B). Collagenase digestion of the adipose tissue, which is validated by F4/80 and adiponectin mRNA expression, revealed that ATF3 is expressed predominantly in stromal-vascular fraction in the adipose tissue (Figure 1C). Furthermore, ATF3 mRNA expression was increased significantly in *ob/ob* mice fed high-fat diet relative to wild-type mice fed standard diet ($P<0.01$) (Figure 1C). We also confirmed by immunostaining of ATF3 and F4/80 using serial sections of obese adipose tissue that most ATF3-positive cells are stained with F4/80 (Figure 1D). These observations indicate that ATF3 is markedly upregulated in obese adipose tissue, especially in infiltrated macrophages.

Saturated Fatty Acids Induce ATF3 via TLR4 in Macrophages In Vitro and In Vivo

We next examined the involvement of TLR4 in the saturated fatty acid–induced ATF3 mRNA and protein expression in macrophages in vitro. Saturated fatty acids, such as palmitate and stearate, and LPS increased significantly ATF3 mRNA and protein expression in RAW264 macrophages ($P<0.05$ versus vehicle) (Figure 2A through 2D). Interestingly, unsaturated fatty acids, such as oleate and eicosapentaenoic acid, did not affect ATF3 mRNA expression (Figure 2C and 2D and data not shown), suggesting the structure-specific effect of free fatty acids. We found that palmitate fails to increase ATF3 mRNA expression in peritoneal macrophages from C3H/HeJ mice with defective TLR4 signaling (Figure 2E). We also observed that BAY11-7085, an NF-κB inhibitor, markedly inhibits the palmitate-induced ATF3 mRNA expression in RAW264 macrophages (Figure 2F). The data were confirmed using RAW264 macrophages overexpressing a super-repressor form of IκBα (SR-IκBα) (Figure 2G). Furthermore, selective NF-κB activation by transient overexpression of p50 and p65 subunits of NF-κB increased significantly the ATF3 promoter activity in HEK293 cells ($P<0.01$) (Figure 2H). In this setting, the changes in ATF3 mRNA expression were almost parallel to those in TNFα mRNA expression (Figure 2E and 2F and data not shown). These observations indicate that TLR4/NF-κB pathway plays an important role in saturated fatty acid–induced ATF3 and TNFα expression in macrophages. On the other hand, palmitate and stearate, but not unsaturated fatty acids, are known to serve as precursors for de novo ceramide synthesis, thereby inducing inflammatory changes in certain cells.[23,24] However, we observed that pharmacological inhibition of ceramide synthesis slightly inhibits the palmitate-induced ATF3

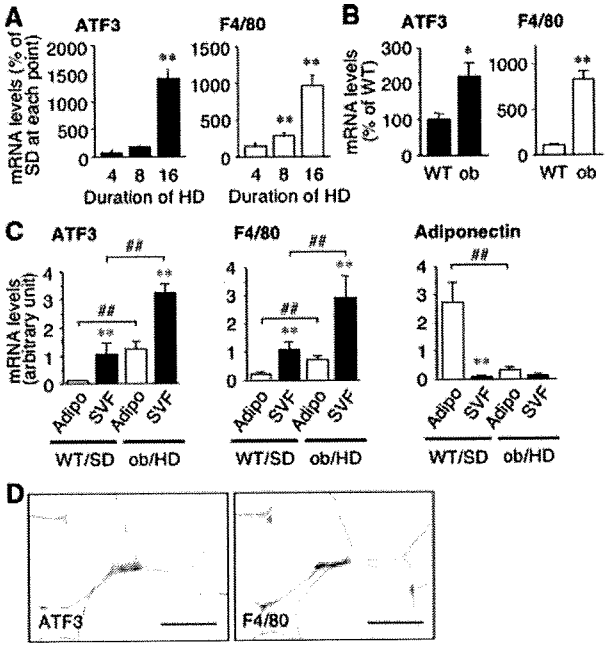

Figure 1. ATF3 expression in obese adipose tissue. ATF3 and F4/80 mRNA expression in the epididymal adipose tissue from high-fat diet (HD)-fed obese mice for up to 16 weeks (A) and genetically obese *ob/ob* mice at 15 weeks of age (ob) (B). *$P<0.05$, **$P<0.01$ vs standard diet (SD) or wild-type mice (WT) (n=6 to 10). C, ATF3, F4/80, and adiponectin mRNA expression in mature adipocytes (Adipo) and stromal-vascular fraction (SVF) in the epididymal adipose tissue from SD-fed WT and HD-fed ob. **$P<0.01$ vs the respective Adipo, ##$P<0.01$ (n=4 to 5). D, ATF3 and F4/80 immunostaining in the epididymal adipose tissue from HD-fed ob. Original magnification, ×400. Scale bars=100 μm.

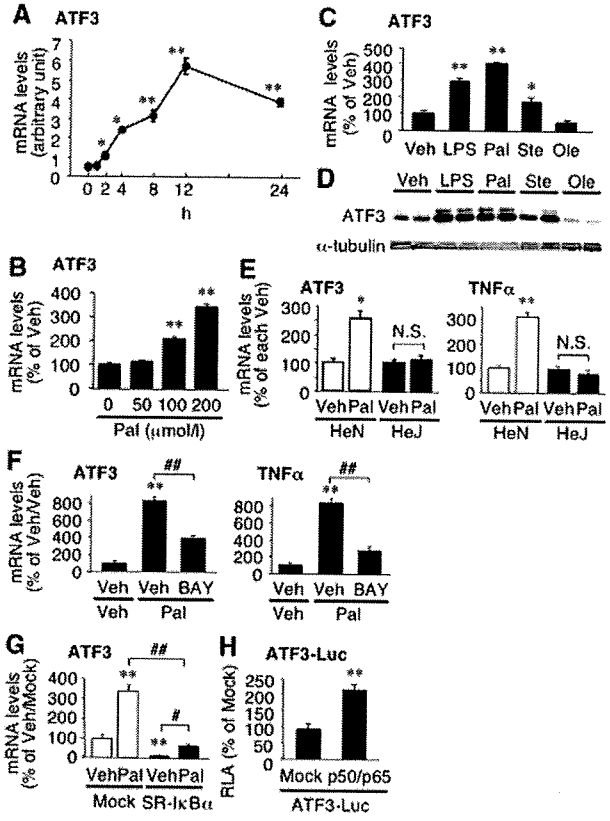

Figure 2. Saturated fatty acid–induced ATF3 expression in cultured macrophages. A, Time course of palmitate-induced ATF3 mRNA expression in RAW264 macrophages. Pal indicates palmitate 200 μmol/L. *$P<0.05$ vs 0 hour. B, Dose-dependent effect of palmitate on ATF3 mRNA expression in RAW264 macrophages. Effect of saturated and unsaturated fatty acids (FAs) on ATF3 mRNA (C) and protein (D) expression in RAW264 macrophages. Veh indicates vehicle; LPS, LPS 10 ng/mL; Pal, palmitate 200 μmol/L; Ste, stearate 200 μmol/L; Ole, oleate 200 μmol/L. *$P<0.05$, **$P<0.01$ vs Veh. E, Role of TLR4 in the palmitate-induced ATF3 and TNFα mRNA expression in peritoneal macrophages. HeN and HeJ indicate peritoneal macrophages from wild-type C3H/HeN and TLR4 mutant C3H/HeJ mice, respectively. *$P<0.05$, **$P<0.01$ vs Veh/HeN. F, Effect of NF-κB inhibitor BAY11-7085 (BAY, 10 μmol/L) on the palmitate-induced ATF3 and TNFα mRNA expression in RAW264 macrophages. **$P<0.01$ vs Veh/Veh, ##$P<0.01$. G, Effect of super-repressor IκBα (SR-IκBα) on the palmitate-induced ATF3 and TNFα mRNA expression in RAW264 macrophages. Mock and SR-IκBα, stably mock-, and SR-IκBα–expressing RAW264 macrophages, respectively. **$P<0.01$ vs Veh/mock; #$P<0.05$, ##$P<0.01$. H, Effect of NF-κB activation on ATF3 promoter activity. The luciferase reporter containing a 1.8-kb human ATF3 promoter fragment (ATF3-Luc) with p50 and p65 subunits of NF-κB or mock was transiently transfected in RAW264 macrophages. **$P<0.01$ vs mock (n=4 to 6).

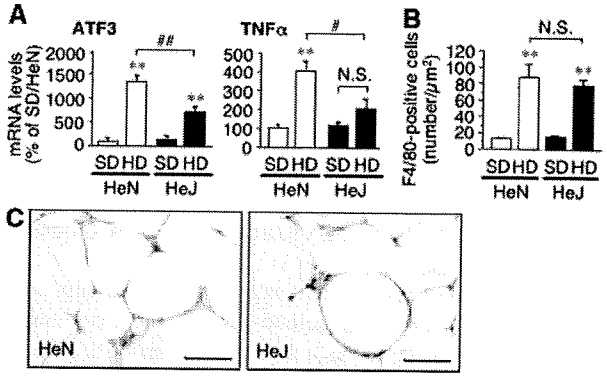

Figure 3. Role of TLR4 in obesity-induced ATF3 mRNA expression in adipose tissue macrophages. ATF3 and TNFα mRNA expression (A) and macrophage infiltration (B) in the adipose tissue from mice fed high-fat diet (HD) or standard diet (SD). **$P<0.01$ vs the respective SD; #$P<0.05$, ##$P<0.01$ (n=6 to 10). C, Immunostaining for ATF3 in the adipose tissue from HD-fed HeN and HeJ. Original magnification, ×400. Scale bars=100 μm.

mRNA expression in RAW264 macrophages (T. Suganami, I. Shirakawa, Y. Ogawa, unpublished data, 2009). These observations, taken together, suggest that saturated fatty acid–induced ATF3 expression is mediated mostly through the TLR4/NF-κB pathway.

We next examined the role of TLR4 in ATF3 expression in the interaction between adipocytes and macrophages. We have established an in vitro coculture system composed of adipocytes and macrophages and found that saturated fatty acids, which are released from adipocytes via the macrophage-induced lipolysis, are capable of activating the TLR4/NF-κB signaling.[6,12] Coculture of 3T3-L1 adipocytes with peritoneal macrophages from C3H/HeN mice resulted in the upregulation of ATF3 and TNFα mRNAs, which was significantly inhibited in the coculture with peritoneal macrophages from C3H/HeJ mice ($P<0.05$) (Online Figure II, a). We found that BAY11-7085 effectively inhibits the upregulation of ATF3 and TNFα mRNA expression in the coculture system (Online Figure II, b).

Using C3H/HeJ and C3H/HeN mice fed high-fat diet, we also examined the involvement of TLR4 in obesity-induced ATF3 expression in the adipose tissue. There were no significant differences in body weight and adipose tissue weight between high-fat diet-fed C3H/HeN and C3H/HeJ mice (Online Table IV). Similar to our previous data on TNFα,[15] the high-fat diet–induced increase in ATF3 mRNA expression was significantly attenuated in the adipose tissue from C3H/HeJ mice relative to C3H/HeN mice ($P<0.01$) (Figure 3A). Importantly, there was no significant change in the number of macrophages infiltrated into the adipose tissue, as assessed by F4/80 immunostaining (Figure 3B), suggesting the attenuation of macrophage activation in C3H/HeJ mice. Immunohistochemical analysis also confirmed the marked reduction of ATF3 staining in C3H/HeJ mice relative to C3H/HeN mice during the high-fat diet (Figure 3C). Collectively, these observations suggest that the saturated fatty acid–induced ATF3 expression in macrophages is mediated via TLR4 in vitro and in vivo.

ATF3 Reduces Saturated Fatty Acid–Induced TNFα Production in Macrophages

To elucidate the functional role of ATF3 in macrophages, we examined the effect of ATF3 overexpression on proinflammatory cytokine production in macrophages in vitro. A full-length mouse ATF3 cDNA was stably overexpressed in RAW264 macrophages by retroviral transduction, which was confirmed by real-time PCR and Western blotting (Figure 4A). In RAW264 macrophages overexpressing ATF3 (ATF3-RAW264), the palmitate- and LPS-induced increase in TNFα

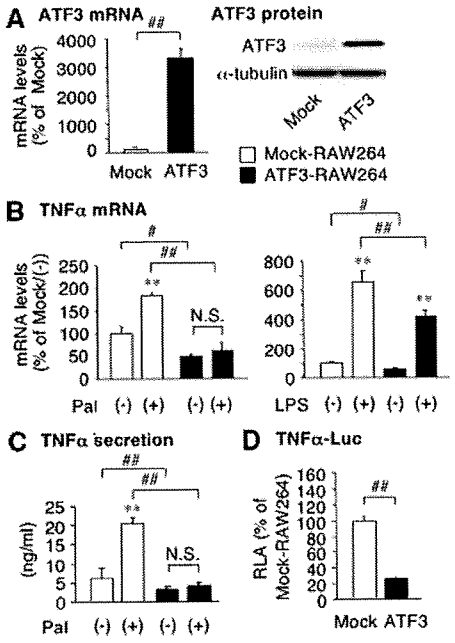

Figure 4. Effect of ATF3 overexpression on saturated fatty acid–induced TNFα production in cultured macrophages. A, Retrovirus-mediated stable overexpression of a full-length mouse ATF3 cDNA in RAW264 macrophages (ATF3-RAW264) and control RAW264 macrophages (Mock-RAW264). Effect of ATF3 overexpression on the palmitate- and LPS-induced TNFα mRNA expression (B) and secretion (C). D, Effect of ATF3 overexpression on the TNFα promoter activity. Pal indicates palmitate 200 μmol/L; LPS, LPS 10 ng/mL. $^{**}P<0.01$ vs the respective control; $\#P<0.05$, $\#\#P<0.01$ (n=4).

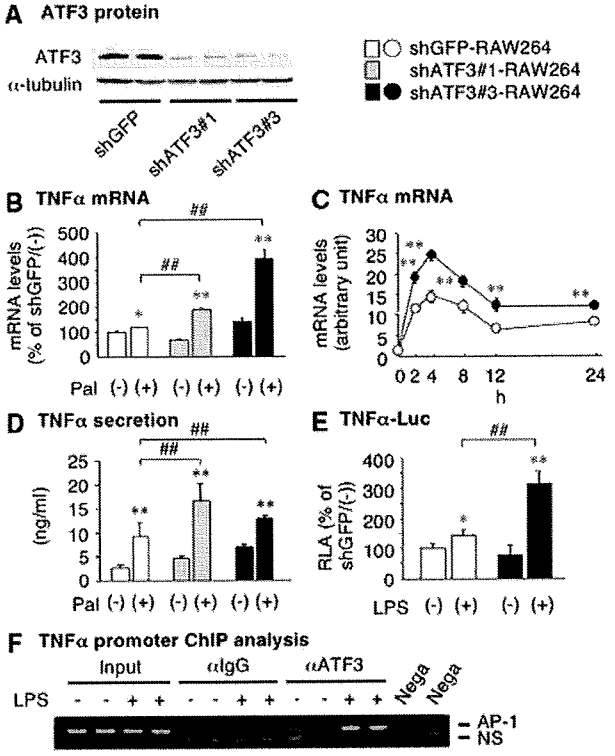

Figure 5. Effect of ATF3 knockdown on saturated fatty acid–induced TNFα production in cultured macrophages. A, Retrovirus-mediated ATF3 knockdown in RAW264 macrophages. Two short hairpin loop RNAs (shATF3#1 and shATF3#3) designed to target different sequences within ATF3 mRNA effectively knocked down endogenous ATF3 in RAW264 macrophages. B, Effect of ATF3 knockdown on the palmitate-induced TNFα mRNA expression. C, Time course of the LPS-induced TNFα mRNA expression in RAW264 macrophages. D, Effect of ATF3 knockdown on the palmitate-induced TNFα secretion. E, Effect of ATF3 knockdown on the TNFα promoter activity. shATF3#1-RAW264 and shATF3#3-RAW264 indicate ATF3–knocked-down RAW264 macrophages; shGFP-RAW264, control RAW264 macrophages; Pal, palmitate 200 μmol/L; LPS, LPS 10 ng/mL. $^{**}P<0.01$ vs the respective control; $\#P<0.05$, $\#\#P<0.01$ (n=4). F, TNFα promoter chromatin immunoprecipitation analysis with chromatin extracts prepared from RAW264 macrophages treated with or without LPS (100 ng/mL) for 6 hours. αATF3 indicates anti-ATF3 antibody; αIgG, normal rabbit IgG; Nega, negative control without template; NS, nonspecific band.

mRNA expression was significantly reduced relative to control RAW264 macrophages (Mock-RAW264) ($P<0.01$) (Figure 4B). We confirmed that the palmitate- and LPS-induced increase in TNFα secretion in the ATF3-RAW264 culture media is significantly reduced relative to Mock-RAW264 ($P<0.01$) (Figure 4C). We also observed with a luciferase reporter assay that TNFα promoter activity is markedly inhibited in ATF3-RAW264 relative to Mock-RAW264 (Figure 4D). Similarly, the palmitate-induced increase in IL-6 and inducible nitric oxide synthase was significantly reduced in ATF3-RAW264 relative to Mock-RAW264 (Online Figure III, a). These observations indicate that overexpression of ATF3 is capable of reducing the saturated fatty acid–induced proinflammatory cytokine production in macrophages.

We next examined the effect of knockdown of endogenous ATF3 gene expression in RAW264 macrophages. Stable knockdown of ATF3 using 2 independent short hairpin loop RNAs (shATF3#1 and shATF3#3) was confirmed by Western blotting (Figure 5A). The ATF3–knocked-down RAW264 macrophages (shATF3#1-RAW264 and shATF3#3-RAW264) exhibited significant enhancement of the palmitate-induced TNFα mRNA expression relative to control RAW264 macrophages (shGFP-RAW264) ($P<0.01$) (Figure 5B). The effect of ATF3 knockdown on TNFα mRNA expression persisted until 24 hours after stimulation with LPS (Figure 5C). Knockdown of ATF3 also significantly increased TNFα secretion in the culture media ($P<0.01$) (Figure 5D). Furthermore, we observed that the TNFα promoter activity is significantly increased in shATF3#3-RAW264 relative to shGFP-RAW264 ($P<0.01$) (Figure 5E). These observations suggest that once induced by the saturated fatty acids/TLR4 signaling, ATF3 attenuates the saturated fatty acid–induced TNFα production in macrophages, thereby constitute a negative feedback mechanism to reduce the TLR4 signaling induction of proinflammatory cytokine production. This notion is consistent with a recent report by Gilchrist et al that ATF3 acts as a negative regulator of the LPS-induced TLR4 signaling.[25]

In the proximal region of the IL-6 and IL-12b promoters, ATF3-binding ATF/CREB sites are located close to NF-κB binding sites.[25] NF-κB and ATF3, both of which are activated by saturated fatty acids/TLR4 signaling, can positively and negatively regulate their target proinflammatory cytokines, respectively.[25] However, there are no consensus sequences

corresponding to the ATF/CREB site close to the NF-κB–binding site (−534 bp) in the proximal region of TNFα promoter. In this study, we performed chromatin immunoprecipitation analysis with RAW264 macrophages and found that ATF3 is recruited to the region containing the activator protein (AP)-1 site (−926 bp) of the endogenous TNFα promoter (Figure 5F). This observation is consistent with a previous report that ATF3 binds to the AP-1 site.[26] It is, therefore, interesting to know how ATF3 negatively regulates TNFα and IL-6 production via its distinct binding sites; the AP-1 and ATF/CREB sites, respectively. In addition, histone deacetylase and heat shock transcription factor 1 are required for the action of ATF3 on the IL-6 promoter.[25,27] It is, therefore, important to identify ATF3-interacting proteins on the TNFα promoter.

Distinct Intracellular Signaling Pathways Plays a Role in the Palmitate- and LPS-Induced ATF3 Expression

In this study, we demonstrated that saturated fatty acids induce ATF3 expression in macrophages through the TLR4/NF-κB pathway, which is consistent with the previous report on LPS.[25] Besides NF-κB, mitogen-activated protein kinases (MAPKs) are an important intracellular signaling pathway downstream of TLR4,[28] and c-Jun N-terminal kinase (JNK) and p38 MAPK have been reported to play a role in ATF3 expression in certain cell types.[29,30] We, therefore, examined the involvement of MAPKs in the saturated fatty acid– and LPS-induced ATF3 mRNA expression and found that SB20358038, a p38 MAPK inhibitor, inhibits significantly the palmitate-induced ATF3 mRNA expression ($P<0.01$) (Online Figure IV). On the other hand, SP600125, a JNK inhibitor, inhibited most effectively the LPS-induced ATF3 mRNA expression ($P<0.01$) (Online Figure IV). Moreover, we found that ERK plays a major role in the palmitate-induced TNFα mRNA expression, whereas other MAPKs may also contribute to the LPS-induced TNFα mRNA expression (Online Figure IV). These observations, taken together, suggest that distinct intracellular signaling pathways may mediate the saturated fatty acid– and LPS-induced ATF3 mRNA expression through TLR4. It is interesting to know how endogenous and exogenous TLR4 ligands such as saturated fatty acids, oxidized phospholipids, and cytosolic and nuclear proteins, and LPS,[12,28,31] exert their effects through the unique signaling pathways, thereby leading to a variety of cellular responses.

Transgenic Overexpression of ATF3 Attenuates Macrophage Activation in Obese Adipose Tissue

To elucidate the role of ATF3 in macrophages infiltrated into obese adipose tissue, we developed transgenic mice overexpressing human ATF3 in macrophages under the control of SR-A promoter (ATF3 Tg) (Online Figure V, a).[32] Genomic Southern blot analysis identified 9 (line 2), 13 (line 25), and 20 (line 35) transgene copies in independent founder lines (data not shown). Western blot analysis of ATF3 revealed 3-fold and 2-fold increase in ATF3 protein levels in bone marrow–derived macrophages from lines 25 and 35, respectively, relative to wild-type mice (Online Figure V, b). In this study, there was no significant increase in ATF3 levels in line 2 macrophages (Online Figure V, b). We observed essentially the same data using peritoneal macrophages from 3 independent transgenic lines (Online Figure V, b).

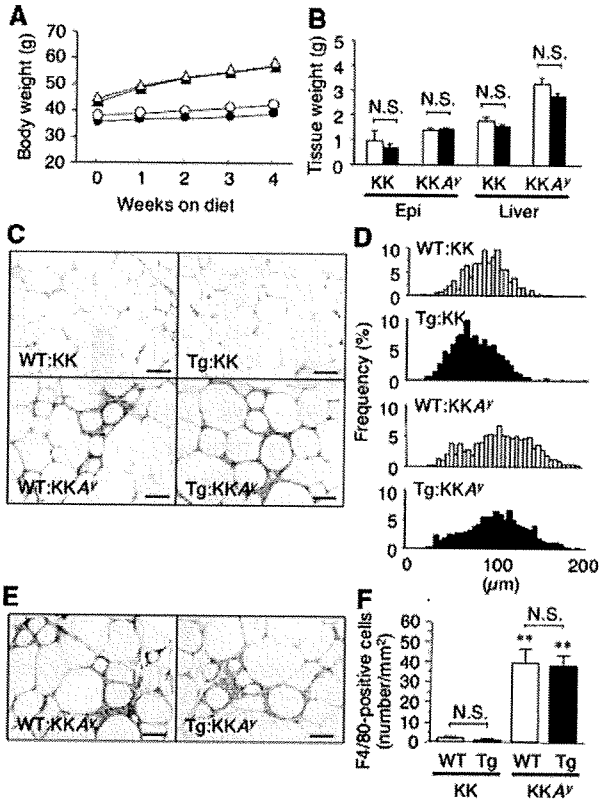

Figure 6. Adipocyte hypertrophy and macrophage infiltration in the adipose tissue from transgenic mice with macrophage-specific ATF3 overexpression. A, Time course of body weight. ○, WT:KK; ●, transgenic (Tg):KK; △, WT:KK*A*^{y}; ▲, Tg:KK*A*^{y}. B, The epididymal adipose tissue (Epi) and liver weights. Open bar, WT; closed bar, Tg. C, Hematoxylin/eosin staining of the epididymal adipose tissue. D, Histogram of diameters of adipocytes in the epididymal adipose tissue. E, F4/80 immunostaining of the epididymal adipose tissue. F, Cell count of F4/80-positive cells in the epididymal adipose tissue. $^{**}P<0.01$ vs the respective KK background (n=6 to 13).

We crossed ATF3 Tg (line 35) with genetically obese KK*A*^{y} mice and obtained 4 genotypes as the F1 generation (wild-type on the KK background [WT:KK], ATF3 Tg on the KK background [ATF3 Tg:KK], wild-type on the KK*A*^{y} background [WT:KK*A*^{y}], and ATF3 Tg on the KK*A*^{y} background [ATF3 Tg:KK*A*^{y}]) at a Mendelian ratio (data not shown). In this study, WT:KK and ATF3 Tg:KK were fed standard diet and WT:KK*A*^{y} and ATF3 Tg:KK*A*^{y} were fed high-fat diet for 4 weeks. During the course of high-fat diet feeding, transgenic overexpression of ATF3 in macrophages did not affect significantly body weight and epididymal fat weight on KK and KK*A*^{y} backgrounds (Figure 6A and 6B). The liver weight tended to be decreased in ATF3 Tg:KK*A*^{y} relative to WT:KK*A*^{y}, but the difference did not reach statistical significance (Figure 6B). Histological analysis showed no apparent difference in adipocyte cell size between genotypes (Figure 6C and 6D). There was no significant difference in obesity-induced macrophage infiltration be-

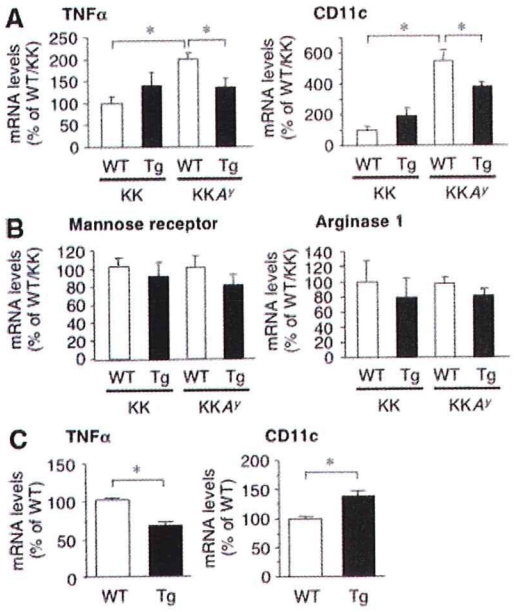

Figure 7. Effect of ATF3 on activation and polarization of adipose tissue macrophages and peritoneal macrophages from macrophage-specific ATF3 transgenic mice. A and B, mRNA expression of M1 markers (TNFα and CD11c) (A) and M2 markers (mannose receptor and arginase 1) (B) in the epididymal adipose tissue from WT:KK, Tg:KK, WT:KKA^y, and Tg:KKA^y mice. C, mRNA expression of M1 markers (TNFα and CD11c) in peritoneal macrophages from WT and Tg on the C57BL/6J background. *P<0.05 (n=6 to 13).

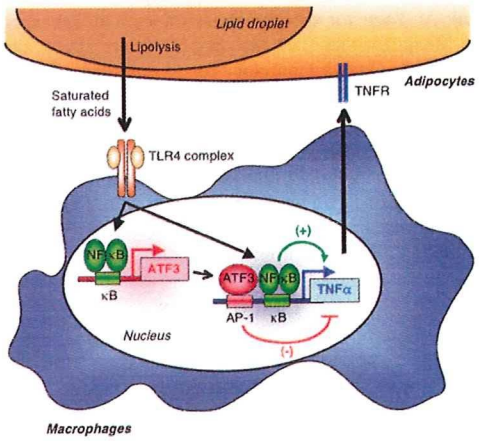

Figure 8. Negative feedback mechanism involving ATF3 as a transcriptional repressor of saturated fatty acid/TLR4 signaling in macrophages in obese adipose tissue. In the interaction between adipocytes and macrophages, ATF3 is upregulated in macrophages through the saturated fatty acids/TLR4/NF-κB signaling. Once induced, ATF3 can transcriptionally reduce the saturated fatty acids/TLR4 signaling–induced proinflammatory cytokine production. Our data have identified ATF3 as a transcriptional repressor of saturated fatty acid/TLR4 signaling, thereby revealing the negative feedback mechanism that attenuates macrophage activation in obese adipose tissue. TNFR indicates TNFα receptor; AP-1 and κB, AP-1– and NF-κB–binding elements, respectively.

tween WT:KKA^y and ATF3 Tg:KKA^y (Figure 6E and 6F). These observations suggest that transgenic overexpression of ATF3 in macrophages does not affect adipocyte hypertrophy and macrophage infiltration in obese adipose tissue.

We also examined the effect of ATF3 on macrophage activation and polarization in the adipose tissue from transgenic mice with macrophage-specific overexpression of ATF3. We observed a marked increase in TNFα mRNA expression in the adipose tissue from WT:KKA^y relative to WT:KK, which was significantly attenuated in ATF3 Tg:KKA^y (P<0.05) (Figure 7A). In this study, M1 macrophage marker CD11c was also increased in the adipose tissue from WT:KKA^y relative to WT:KK (Figure 7B), which was effectively inhibited in ATF3 Tg:KKA^y (P<0.05) (Figure 7A). Moreover, IL-6 mRNA expression tended to be decreased in the adipose tissue from ATF3 Tg:KKA^y mice relative to WT:KKA^y (Online Figure III, b). By contrast, we found no significant difference in mRNA expression of M2 macrophage markers, mannose receptor and arginase 1, among genotypes (Figure 7B). These observations suggest that overexpression of ATF3 in macrophages is capable of inhibiting macrophage activation and M1 polarization in the adipose tissue in vivo (Figure 8).

We next examined TNFα and CD11c mRNA expression in peritoneal macrophages prepared from ATF3 Tg and WT on the C57BL/6J background. Similar to the data on the adipose tissue (Figure 7A), TNFα mRNA expression was significantly suppressed in peritoneal macrophages from ATF3 Tg relative to WT (P<0.05) (Figure 7C). Interestingly, CD11c mRNA expression in peritoneal macrophages was rather higher in ATF3 Tg than in WT (P<0.05) (Figure 7C). In this regard, using ATF3-RAW264 and shATF3-RAW264, we did not observe that ATF3 has impact on CD11c mRNA expression in vitro (data not shown), suggesting that CD11c may not be a transcriptional target of ATF3 in macrophages. Further studies are needed to elucidate the role of ATF3 in obesity-induced M1 polarization of adipose tissue macrophages. Global ATF3-deficient mice are viable,[19,25] but the role of ATF3 in glucose/lipid metabolism has not been elucidated. Because activation and polarization of adipose tissue macrophages play an important role in the metabolic status,[7–9] studies with ATF3 Tg and macrophage-specific ATF3-deficient mice would help elucidate the pathophysiologic role of ATF3 in macrophages in adipose tissue inflammation and systemic glucose/lipid metabolism.

In conclusion, ATF3 is upregulated in macrophages in the interaction between adipocytes and macrophages through the saturated fatty acids/TLR4/NF-κB signaling. Once induced, ATF3 can transcriptionally reduce the saturated fatty acids/TLR4 signaling induction of proinflammatory cytokine production. Among known negative regulators of TLR4 signaling,[28] ATF3 is unique in that it represses the TLR4 target genes via a transcriptional mechanism. This study provides evidence that ATF3 acts as a transcriptional repressor of saturated fatty acids/TLR4 signaling, thereby revealing the negative feedback mechanism that attenuates macrophage activation in obese adipose tissue (Figure 8). Our data also suggest that activation of ATF3 in macrophages may offer a novel therapeutic strategy to prevent or treat obesity-induced adipose tissue inflammation.

Acknowledgments

We thank Ai Togo for secretarial assistance and Takanori Kunieda and Tae Mieda for technical assistance. We are also grateful to the members of the Ogawa laboratory for discussions.

Sources of Funding

This work was supported in part by a Grant-in-Aid for Scientific Research from the Ministry of Education, Culture, Sports, Science and Technology of Japan and Ministry of Health, Labor and Welfare of Japan and research grants from Takeda Science Foundation and Takeda Medical Research Foundation.

Disclosures

None.

References

1. Grundy SM, Brewer HB, Jr, Cleeman JI, Smith SC Jr, Lenfant C. Definition of metabolic syndrome: report of the National Heart, Lung, and Blood Institute/American Heart Association conference on scientific issues related to definition. *Circulation*. 2004;109:433–438.
2. Hotamisligil GS. Inflammation and metabolic disorders. *Nature*. 2006; 444:860–867.
3. Berg AH, Scherer PE. Adipose tissue, inflammation, and cardiovascular disease. *Circ Res*. 2005;96:939–949.
4. Matsuzawa Y, Funahashi T, Nakamura T. Molecular mechanism of metabolic syndrome X: contribution of adipocytokines adipocyte-derived bioactive substances. *Ann N Y Acad Sci*. 1999;892:146–154.
5. Weisberg SP, McCann D, Desai M, Rosenbaum M, Leibel RL, Ferrante AW Jr. Obesity is associated with macrophage accumulation in adipose tissue. *J Clin Invest*. 2003;112:1796–1808.
6. Suganami T, Nishida J, Ogawa Y. A paracrine loop between adipocytes and macrophages aggravates inflammatory changes: role of free fatty acids and tumor necrosis factor α. *Arterioscler Thromb Vasc Biol*. 2005; 25:2062–2068.
7. Lumeng CN, Bodzin JL, Saltiel AR. Obesity induces a phenotypic switch in adipose tissue macrophage polarization. *J Clin Invest*. 2007;117: 175–184.
8. Kang K, Reilly SM, Karabacak V, Gangl MR, Fitzgerald K, Hatano B, Lee CH. Adipocyte-derived Th2 cytokines and myeloid PPARδ regulate macrophage polarization and insulin sensitivity. *Cell Metab*. 2008;7: 485–495.
9. Odegaard JI, Ricardo-Gonzalez RR, Red Eagle A, Vats D, Morel CR, Goforth MH, Subramanian V, Mukundan L, Ferrante AW, Chawla A. Alternative M2 activation of Kupffer cells by PPARδ ameliorates obesity-induced insulin resistance. *Cell Metab*. 2008;7:496–507.
10. Cao H, Gerhold K, Mayers JR, Wiest MM, Watkins SM, Hotamisligil GS. Identification of a lipokine, a lipid hormone linking adipose tissue to systemic metabolism. *Cell*. 2008;134:933–944.
11. Unger RH. Lipotoxicity in the pathogenesis of obesity-dependent NIDDM. Genetic and clinical implications. *Diabetes*. 1995;44:863–870.
12. Suganami T, Tanimoto-Koyama K, Nishida J, Itoh M, Yuan X, Mizuarai S, Kotani H, Yamaoka S, Miyake K, Aoe S, Kamei Y, Ogawa Y. Role of the Toll-like receptor 4/NF-κB pathway in saturated fatty acid-induced inflammatory changes in the interaction between adipocytes and macrophages. *Arterioscler Thromb Vasc Biol*. 2007;27:84–91.
13. Lee JY, Sohn KH, Rhee SH, Hwang D. Saturated fatty acids, but not unsaturated fatty acids, induce the expression of cyclooxygenase-2 mediated through Toll-like receptor 4. *J Biol Chem*. 2001;276: 16683–16689.
14. Shi H, Kokoeva MV, Inouye K, Tzameli I, Yin H, Flier JS. TLR4 links innate immunity and fatty acid-induced insulin resistance. *J Clin Invest*. 2006;116:3015–3025.
15. Suganami T, Mieda T, Itoh M, Shimoda Y, Kamei Y, Ogawa Y. Attenuation of obesity-induced adipose tissue inflammation in C3H/HeJ mice carrying a Toll-like receptor 4 mutation. *Biochem Biophys Res Commun*. 2007;354:45–49.
16. Poggi M, Bastelica D, Gual P, Iglesias MA, Gremeaux T, Knauf C, Peiretti F, Verdier M, Juhan-Vague I, Tanti JF, Burcelin R, Alessi MC. C3H/HeJ mice carrying a Toll-like receptor 4 mutation are protected against the development of insulin resistance in white adipose tissue in response to a high-fat diet. *Diabetologia*. 2007;50:1267–1276.
17. Tsukumo DM, Carvalho-Filho MA, Carvalheira JB, Prada PO, Hirabara SM, Schenka AA, Araujo EP, Vassallo J, Curi R, Velloso LA, Saad MJ. Loss-of-function mutation in Toll-like receptor 4 prevents diet-induced obesity and insulin resistance. *Diabetes*. 2007;56:1986–1998.
18. Cai Y, Zhang C, Nawa T, Aso T, Tanaka M, Oshiro S, Ichijo H, Kitajima S. Homocysteine-responsive ATF3 gene expression in human vascular endothelial cells: activation of c-Jun NH_2-terminal kinase and promoter response element. *Blood*. 2000;96:2140–2148.
19. Hartman MG, Lu D, Kim ML, Kociba GJ, Shukri T, Buteau J, Wang X, Frankel WL, Guttridge D, Prentki M, Grey ST, Ron D, Hai T. Role for activating transcription factor 3 in stress-induced beta-cell apoptosis. *Mol Cell Biol*. 2004;24:5721–5732.
20. Poltorak A, He X, Smirnova I, Liu MY, Van Huffel C, Du X, Birdwell D, Alejos E, Silva M, Galanos C, Freudenberg M, Ricciardi-Castagnoli P, Layton B, Beutler B. Defective LPS signaling in C3H/HeJ and C57BL/10ScCr mice: mutations in TLR4 gene. *Science*. 1998;282:2085–2088.
21. Kitagawa K, Wada T, Furuichi K, Hashimoto H, Ishiwata Y, Asano M, Takeya M, Kuziel WA, Matsushima K, Mukaida N, Yokoyama H. Blockade of CCR2 ameliorates progressive fibrosis in kidney. *Am J Pathol*. 2004;165:237–246.
22. Tamura K, Hua B, Adachi S, Guney I, Kawauchi J, Morioka M, Tamamori-Adachi M, Tanaka Y, Nakabeppu Y, Sunamori M, Sedivy JM, Kitajima S. Stress response gene ATF3 is a target of c-myc in serum-induced cell proliferation. *EMBO J*. 2005;24:2590–2601.
23. Shulman GI. Cellular mechanisms of insulin resistance. *J Clin Invest*. 2000;106:171–176.
24. Haversen L, Danielsson KN, Fogelstrand L, Wiklund O. Induction of proinflammatory cytokines by long-chain saturated fatty acids in human macrophages. *Atherosclerosis*. 2009;202:382–393.
25. Gilchrist M, Thorsson V, Li B, Rust AG, Korb M, Roach JC, Kennedy K, Hai T, Bolouri H, Aderem A. Systems biology approaches identify ATF3 as a negative regulator of Toll-like receptor 4. *Nature*. 2006;441:173–178.
26. Kim HB, Kong M, Kim TM, Suh YH, Kim WH, Lim JH, Song JH, Jung MH. NFATc4 and ATF3 negatively regulate adiponectin gene expression in 3T3–L1 adipocytes. *Diabetes*. 2006;55:1342–1352.
27. Inouye S, Fujimoto M, Nakamura T, Takaki E, Hayashida N, Hai T, Nakai A. Heat shock transcription factor 1 opens chromatin structure of interleukin-6 promoter to facilitate binding of an activator or a repressor. *J Biol Chem*. 2007;282:33210–33217.
28. Akira S, Takeda K. Toll-like receptor signalling. *Nat Rev Immunol*. 2004;4:499–511.
29. Lim JH, Lee JI, Suh YH, Kim W, Song JH, Jung MH. Mitochondrial dysfunction induces aberrant insulin signalling and glucose utilisation in murine C2C12 myotube cells. *Diabetologia*. 2006;49:1924–1936.
30. Lu D, Chen J, Hai T. The regulation of ATF3 gene expression by mitogen-activated protein kinases. *Biochem J*. 2007;401:559–567.
31. Imai Y, Kuba K, Neely GG, Yaghubian-Malhami R, Perkmann T, van Loo G, Ermolaeva M, Veldhuizen R, Leung YH, Wang H, Liu H, Sun Y, Pasparakis M, Kopf M, Mech C, Bavari S, Peiris JS, Slutsky AS, Akira S, Hultqvist M, Holmdahl R, Nicholls J, Jiang C, Binder CJ, Penninger JM. Identification of oxidative stress and Toll-like receptor 4 signaling as a key pathway of acute lung injury. *Cell*. 2008;133:235–249.
32. Horvai A, Palinski W, Wu H, Moulton KS, Kalla K, Glass CK. Scavenger receptor A gene regulatory elements target gene expression to macrophages and to foam cells of atherosclerotic lesions. *Proc Natl Acad Sci U S A*. 1995;92:5391–5395.

Expanded Materials and Methods

Materials and Antibodies

NF-κB inhibitor BAY11-7085, p38 MAPK inhibitor SB203580, and JNK inhibitor SP600125 were purchased from Merck (San Diego, CA). MEK inhibitor U0126 was purchased from Cell Signaling Technology (Danvers, MA). The pEF-p50-NHA and pEF-p60 plasmids which express p50 and p65 subunits of NF-κB, respectively, and the pMRX-SR-IκBα plasmid which expresses a super-repressor form of IκBα (SR-IκBα; a degradation- resistant mutant of IκBα) are described elsewhere.[1, 2] LPS (from Escherichia. coli O111: B4) and anti-α-tubulin antibody were purchased from Sigma (San Diego, CA). Palmitate, stearate, and oleate were purchased from Sigma, solubilized in ethanol, and conjugated with fatty acids- and immunoglobulin-free bovine serum albumin (Sigma) at a molar ratio of 10: 1 (fatty acid: albumin) in low serum medium as previously described.[3] The concentrations of palmitate used in this study (< 200 μmol/l) are within the physiologic levels. Antibody against ATF3 was purchased from Santa Cruz (sc-188, Santa Cruz, CA). All other reagents were purchased from Sigma or Nacalai Tesque (Kyoto, Japan) unless otherwise described.

cDNA Microarray Analysis

Serum starved RAW264 macrophages were treated with palmitate (200 μmol/l) or vehicle for 5 h. The epididymal adipose tissue was prepared from 12-week-old male *ob/ob* and wild-type mice. DNA microarray analysis was performed as previously described.[4] In brief, total RNA was extracted using TRIzol reagent (Invitrogen, Carlsbad, CA) and repurified with an RNeasy purification kit (Qiagen, Hilden, Germany). Ten μg of RNA was applied for microarray analysis (Mouse Genome 430A 2.0; Affymetrix, Santa Clara, CA) and GeneChip software (Affymetrix) was utilized for analysis of microarray data.

Co-culture of Adipocytes and Macrophages

Co-culture of adipocytes and macrophages was performed as described.[3, 4] In brief, serum starved differentiated 3T3-L1 adipocytes (~0.5 x 10^6 cells) were cultured in a 35-mm dish and

macrophages (1.0 x 10^5 cells of RAW264 macrophages or peritoneal macrophages) were plated onto 3T3-L1 adipocytes. The cells were cultured for 24 h with contact each other and harvested. As a control, adipocytes and macrophages, the numbers of which were equal to those in the co-culture, were cultured separately and mixed after harvest.

Animals

Six-week-old male C3H/HeJ mice which have defective LPS signaling due to a missense mutation in the TLR4 gene[5] and control C3H/HeN mice were purchased from CLEA Japan (Tokyo, Japan). Genetically obese *ob/ob*, *db/db*, and KKA^y mice were purchased from CLEA Japan and Charles River Japan (Tokyo, Japan). The animals were housed in individual cages in a temperature-, humidity-, and light-controlled room (12-h light and 12-h dark cycle) and allowed free access to water and standard chow (Oriental MF; 362 kcal/100 g, 5.4% energy as fat) (Oriental Yeast, Tokyo, Japan), when otherwise noted. In the high-fat feeding experiments, male mice at 10 weeks of age were given free access to water and either the standard chow or high-fat diet (D12492; 556 kcal/100g, 60% energy as fat; Research Diets, New Brunswick, NJ) for 4 weeks.[6] At the end of the experiments, mice were sacrificed after a 1-h fast under intraperitoneal pentobarbital anesthesia (30 mg/kg). All animal experiments were conducted in accordance to the guidelines of Tokyo Medical and Dental University Committee on Animal Research (No. 0090058).

Generation of Transgenic Mice Overexpressing ATF3 in Macrophages

The 4.96-kb enhancer/promoter of the human scavenger receptor-A (SR-A) gene capable of macrophage-specific expression was kindly provided by Dr. Christopher K. Glass (University of California, San Diego, CA).[7] A full-length human ATF3 cDNA was fused with SR-A enhancer/promoter and a human growth hormone polyadenylation site. The transgene (Online Figure Va) was linearized and microinjected into the pronuclei of C57BL/6J mouse fertilized eggs. To identify founder mouse lines that carried the SR-A enhancer/promoter-ATF3 transgene, Southern blot analysis was performed using tail tissue DNA. Expression of ATF3

mRNA and protein in peritoneal and bone marrow-derived macrophages was evaluated by real-time PCR and Western blotting, respectively.

Chromatin Immunoprecipitation (ChIP) Assay

To assess ATF3 binding to the TNFα promoter, ChIP assay was performed using the ChIP assay kit (Upstate Biotechnology, CA) according to the manufacture's instruction[8]. After stimulation with LPS, cells were fixed in 1% formaldehyde for 15 min at 37°C to cross-link DNA and proteins, lysed, and sheared with a handy sonicator (Tomy Seiko, Tokyo, Japan) to generate DNA ranging in size from 200 to 1000 bp. The lysates were pre-cleared with protein A-agarose and immunoprecipitated by incubating overnight at 4°C with anti-ATF3 antibody (Sant Cruz) or normal rabbit IgG as a negative control. Before immunoprecipitation, "input" samples were removed from the lysates. After immunoprecipitation, protein-DNA complexes were eluted in a buffer containing 1% SDS and 0.1 M $NaHCO_3$, and the cross-links were reversed. The resulting DNA was purified by phenol/chloroform extraction and ethanol precipitation, and subjected to semiquantitative PCR analysis.

The primers used for PCR were designed to amplify the proximal sequence of the mouse TNFα promoter containing the AP-1 site at -926 bp relative to the transcription start site (NM_013693): forward (5'-CAGAGACATGGTGGATTCACG-3') and reverse (5'-GCCCTGCTTCCAGGATTTCTC -3').

Retrovirus-mediated Overexpression and Knockdown of ATF3 in Macrophages

A full-length mouse ATF3 cDNA, consisting of 543 bp encoding 181 amino acid residues, was amplified by PCR with a pair of primers, one with a BamHI site and the other with an EcoRI site at the terminus. The PCR product was inserted into the BamHI/EcoRI cloning sites of the pMRX retroviral vector.[9] The retroviral expression vector (pMRX-mATF3) capable of expressing mouse ATF3 ORF was transfected into Plat-E packaging cells[9, 10] and the retrovirus was harvested 48 h to 72 h after transfection.[11] RAW264 cells were infected with the viral supernatant for 4 h and then cultured in medium supplemented with 10% fetal bovine

serum before selection. Puromycin (5 μg/ml) was added to the medium 2 days after the initial infection and the selection was continued for 2 weeks. Stable ATF3-RAW264 cell line was obtained after evaluating the expression levels of ATF3 protein by Western blotting.

pSINsi-hU6 DNA (Code 3661, Takara Bio, Otsu, Japan) for the synthesis of siRNA under the control of the human U6 promoter was used to generate pshATF3 plasmids expressing hairpin RNAs of ATF3 target sequences. The resulting pshATF3#1 and pshATF3#3, synthesizing sequences corresponding to nt 745-763 (5'-GGAACCTCTTTATCCAACA-3') and nt 989-1007 (5'-GCATCCTTTGTCTCACCAA-3'), respectively, of mouse ATF3 mRNA (NM_007498) were used for knockdown of endogenous ATF3. As a control, pshGFP was constructed in the same way and the sequence used to target the GFP gene was as described elsewhere.[12] Retrovirus preparation and RAW264 cell infection are the same as described above except that the selection is under G418 (400 μg/ml, Invitrogen, Carlsbad, CA). Stable shATF3-Raw264 cell line was verified for the knockdown efficiency by Western blotting.

Transient Transfection and Luciferase Assay

A luciferase reporter assay was performed as previously described[4] using the luciferase reporter constructs for ATF3 and TNFα promoters.[13] The luciferase reporter construct with no cis-acting DNA elements was used as a negative control. In brief, RAW264 macrophages or HEK293 cells were transiently transfected by electroporation (Nucleofector system; Amaxa, Gaithersburg, MD) or lipofectamine 2000 (Invitrogen), with a luciferase reporter vector and pRL-TK vector (Promega, Madison, WI) as an internal control for transfection efficiency. The luciferase activity was determined using the Dual-Luciferase Reporter Assay System (Promega).

References

1. Tomita S, Fujita T, Kirino Y, Suzuki T. PDZ domain-dependent suppression of NF-κB/p65-induced Aβ42 production by a neuron-specific X11-like protein. *J Biol Chem.* 2000;275:13056-13060.
2. Hironaka N, Mochida K, Mori N, Maeda M, Yamamoto N, Yamaoka S. Tax-independent constitutive IκB kinase activation in adult T-cell leukemia cells. *Neoplasia.* 2004;6:266-278.
3. Suganami T, Nishida J, Ogawa Y. A paracrine loop between adipocytes and macrophages aggravates inflammatory changes: role of free fatty acids and tumor necrosis factor α. *Arterioscler Thromb Vasc Biol.* 2005;25:2062-2068.
4. Suganami T, Tanimoto-Koyama K, Nishida J, Itoh M, Yuan X, Mizuarai S, Kotani H, Yamaoka S, Miyake K, Aoe S, Kamei Y, Ogawa Y. Role of the Toll-like receptor 4/NF-κB pathway in saturated fatty acid-induced inflammatory changes in the interaction between adipocytes and macrophages. *Arterioscler Thromb Vasc Biol.* 2007;27:84-91.
5. Poltorak A, He X, Smirnova I, Liu MY, Van Huffel C, Du X, Birdwell D, Alejos E, Silva M, Galanos C, Freudenberg M, Ricciardi-Castagnoli P, Layton B, Beutler B. Defective LPS signaling in C3H/HeJ and C57BL/10ScCr mice: mutations in TLR4 gene. *Science.* 1998;282:2085-2088.
6. Suganami T, Mieda T, Itoh M, Shimoda Y, Kamei Y, Ogawa Y. Attenuation of obesity-induced adipose tissue inflammation in C3H/HeJ mice carrying a Toll-like receptor 4 mutation. *Biochem Biophys Res Commun.* 2007;354:45-49.
7. Horvai A, Palinski W, Wu H, Moulton KS, Kalla K, Glass CK. Scavenger receptor A gene regulatory elements target gene expression to macrophages and to foam cells of atherosclerotic lesions. *Proc Natl Acad Sci U S A.* 1995;92:5391-5395.
8. Kamei Y, Miura S, Suganami T, Akaike F, Kanai S, Sugita S, Katsumata A, Aburatani H, Unterman TG, Ezaki O, Ogawa Y. Regulation of SREBP1c gene expression in skeletal

muscle: role of retinoid X receptor/liver X receptor and forkhead-O1 transcription factor. *Endocrinology.* 2008;149:2293-2305.

9. Saitoh T, Nakayama M, Nakano H, Yagita H, Yamamoto N, Yamaoka S. TWEAK induces NF-κB2 p100 processing and long lasting NF-κB activation. *J Biol Chem.* 2003;278:36005-36012.
10. Morita S, Kojima T, Kitamura T. Plat-E: an efficient and stable system for transient packaging of retroviruses. *Gene Ther.* 2000;7:1063-1066.
11. Ito A, Suganami T, Miyamoto Y, Yoshimasa Y, Takeya M, Kamei Y, Ogawa Y. Role of MAPK phosphatase-1 in the induction of monocyte chemoattractant protein-1 during the course of adipocyte hypertrophy. *J Biol Chem.* 2007;282:25445-25452.
12. Caplen NJ, Parrish S, Imani F, Fire A, Morgan RA. Specific inhibition of gene expression by small double-stranded RNAs in invertebrate and vertebrate systems. *Proc Natl Acad Sci U S A.* 2001;98:9742-9747.
13. Cai Y, Zhang C, Nawa T, Aso T, Tanaka M, Oshiro S, Ichijo H, Kitajima S. Homocysteine-responsive ATF3 gene expression in human vascular endothelial cells: activation of c-Jun NH_2-terminal kinase and promoter response element. *Blood.* 2000;96:2140-2148.

Online Figure Legends

Online Figure I. Identification of ATF3 as a Target Gene of Saturated Fatty Acid in Obese Adipose Tissue. (a) cDNA microarray analysis screening for a target of saturated fatty acid/TLR4 signaling in obese adipose tissue. RAW264 macrophages were treated with either palmitate (200 μmol/l) or vehicle for 5 h. The epididymal adipose tissue was prepared from 12-week-old male *ob/ob* or wild-type mice. (b) Tissue distribution of ATF3 and F4/80 mRNAs in mice. WAT, white adipose tissue. Open and closed bars indicate wild-type mice fed standard diet and *db/db* mice fed high-fat diet, respectively. $*P < 0.01$ vs. wild-type mice fed standard diet. $n = 4$-6.

Online Figure II. Role of the TLR4/NF-κB Signaling in ATF3 mRNA Expression in the Interaction between Adipocytes and Macrophages. (a) ATF3 and TNFα mRNA expression in the co-culture between 3T3-L1 adipocytes and peritoneal macrophages obtained from C3H/HeN mice (HeN) or C3H/HeJ mice (HeJ). ct, control culture; co, co-culture. $*P < 0.05$, $**P < 0.01$ vs. the respective ct; $\#P < 0.05$. $n = 4$. (b) Role of NF-κB in the co-culture-induced ATF3 and TNFα mRNA expression. Co-culture was performed using 3T3-L1 adipocytes and RAW264 macrophages. BAY, BAY11-7085 10 μmol/l. $*P < 0.05$, $**P < 0.01$ vs. Veh/ct; $\#P < 0.05$, $\#\#P < 0.01$. $n = 4$.

Online Figure III. Effect of ATF3 Overexpression on IL-6 and iNOS mRNA Expression *in vitro* and *in vivo*. (a) Effect of ATF3 on the palmitate-induced IL-6 and iNOS mRNA expression in RAW264 macrophages overexpressing ATF3 (ATF3) and control RAW264 macrophages (Mock). (b) IL-6 and iNOS mRNA expression in the adipose tissue from WT:KK, Tg:KK, WT:KKA^y, and Tg:KKA^y mice. Veh, vehicle; Pal, palmitate 200 μmol/l; WT, wild-type; Tg, ATF3 transgenic mice. $**P < 0.01$ vs. Veh/Mock; $\#\#P < 0.01$. $n = 4$.

Online Figure IV. Effect of MAPK Inhibitors on Palmitate- and LPS-induced ATF3 and TNFα mRNA Expression in RAW264 Macrophages. Veh, vehicle; Pal, palmitate

100 μmol/l; LPS, LPS 10 ng/ml; U, U0126 5 μmol/l; SP, SP600125 10 μmol/l; SB, SB203580 10 μmol/l. $^{**}P < 0.01$ vs. Veh/Veh, $\#\#P < 0.01$. $n = 4$.

Online Figure V. Generation of Transgenic Mice Overexpressing ATF3 in Macrophages. (a) Schematic representation of the mouse SR-A promoter/human ATF3 fusion gene. (b) Western blot analysis of ATF3 protein expression in peritoneal macrophages and bone marrow-derived macrophages obtained from three independent transgenic lines (#2, #25, #35) and wild-type mice.

Online Table I. Primers used in this study.

Genes	Primers
Adiponectin	Fw: 5'-ATGGCAGAGATGGCACTCCT-3'
	Rv: 5'-CCTTCAGCTCCTGTCATTCCA-3'
Arginase 1	Fw: 5'-CTCCAAGCCAAAGTCCTTAGAG-3'
	Rv: 5'-AGGAGCTGTCATTAGGGACATC-3'
ATF3	Fw: 5'-TGCCTGCAGAAAGAGTCAGAGA -3'
	Rv: 5'-AGCTCCTCGATCTGGGCC-3'
CD11c	Fw: 5'-CTGGATAGCCTTTCTTCTGCTG -3'
	Rv: 5'-GCACACTGTGTCCGAACTC-3'
F4/80	Fw: 5'-CTTTGGCTATGGGCTTCCAGTC-3'
	Rv: 5'-GCAAGGAGGACAGAGTTTATCGTG-3'
IL-6	Fw: 5'-ACAACCACGGCCTTCCCTACTT-3'
	Rv: 5'-CACGATTTCCCAGAGAACATGTG-3'
iNOS	Fw: 5'- CCAAGCCCTCACCTACTTCC-3'
	Rv: 5'- CTCTGAGGGCTGACACAAGG-3'
Mannose receptor	Fw: 5'- CGGTGAACCAAATAATTACCAAAAT-3'
	Rv: 5'-GTGGAGCAGGTGTGGGCT-3'
TNFα	Fw: 5'- ACCCTCACACTCAGATCATCTTC-3'
	Rv: 5'- TGGTGGTTTGCTACGACGT-3'
36B4	Fw: 5'-GGCCCTGCACTCTCGCTTTC-3'
	Rv: 5'-TGCCAGGACGCGCTTGT-3'